Rock Mech Rock Eng (2017) 50:225–232
DOI 10.1007/s00603-016-1050-9

TECHNICAL NOTE

Microseismic Monitoring of the Left Bank Slope at the Baihetan Hydropower Station, China

Feng Dai[1] · Biao Li[1] · Nuwen Xu[1] · Guotao Meng[2] · Jiayao Wu[2] · Yilin Fan[3]

Received: 28 December 2015 / Accepted: 9 July 2016 / Published online: 15 July 2016

Keywords Rock slope · Microseismic monitoring · Field observation · Baihetan hydropower station

1 Introduction

Layered rock slopes are especially prone to collapse under excavation excitations due to the relatively weak strength characteristics of discontinuities such as joints, bedding planes and foliations (Liu et al. 2004, 2014). The stability analysis of layered rock slopes is of increased importance when subjected to continuous excavation. A systematic study and analysis of high rock slope stability has been performed in related studies (Stacey et al. 2004; Stead et al. 2006; Stead and Wolter 2015). However, approaches are rare that have already formed mature programmes and that have been effectively used in engineering practices. Compared with theoretical and numerical studies, field monitoring provides an actual and visual approach to the study of the deformation failure characteristics of rock slopes, especially for complicated cases (i.e., deep interlayer staggered zones and intraformational faulted zones) where theoretical or numerical solutions are difficult to obtain. Traditional measurement techniques, such as multiple-point extensometers, anchor stress gauges and global positioning system, are useful for monitoring the surface deformation. However, they are unrealistic to effectively monitor the microcracking activities in rock masses prior to the formation of macroscopic fractures on slope surface.

In general, macro-fractures and deformation failure in the rock mass often lag behind the initiation, coalescences and propagation of microcracks. Thus, there must be an intrinsic correlation between micro-fractures (microseismicity) and rock slope instability (Xu et al. 2012). Although it is difficult to monitor the full-field stress, the response of the rock slope to stresses (i.e., microcracking) can be monitored. The variation of stress due to engineering excavation can be indirectly obtained through monitoring the microcracking evolution. The microseismic (MS) monitoring technique can help to achieve this goal (Kaiser 2009; Tang et al. 2011). More descriptions about the principle and applications of MS monitoring technique were detailed in related studies (Cai et al. 2001; Hirata et al. 2007; Hudyma and Potvin 2010; Trifu and Shumila 2010; Xu et al. 2014, 2016; Young et al. 2004).

2 Site Characterization of the Left Bank Slope

2.1 Project Overview and Geological Settings

The Baihetan hydropower station is a large-scale step hydropower project recently constructed on the Jinshajiang River in southwest China (Wang et al. 2015). The left bank is the southeast slope of Daliang Mountain, with a peak height of 2600 m, and it has a sloped terrain generally inclined toward the Jinshajiang River. The left bank abutment has an approximate SN direction, inclining to the east

✉ Nuwen Xu
xunuwen@scu.edu.cn

[1] State Key Laboratory of Hydraulics and Mountain River Engineering, College of Water Resource and Hydropower, Sichuan University, Chengdu 610065, Sichuan Province, People's Republic of China

[2] HydroChina-Itasca R&D Center, Hangzhou 310014, Zhejiang Province, People's Republic of China

[3] China Three Gorges Corporation, Beijing 100038, People's Republic of China

with a 60° slope. The left bank slope is a bedding slope with an attitude of N30–50°E and SE ∠15–25°. There are many interlayer staggered zones (i.e., C3 and C3-1, where the occurrence of C3 is N35–50°E and SE ∠15–20°) and faults with high deep angles in the NE direction (i.e., F17, F16 and F14). The interlayer staggered zones (i.e., LS412, LS415 and LS423) and faults (i.e., f108 and f110) along the NW direction develop at the elevations of 834–750 m. The interlayer staggered zone LS411 and the interlamination staggered zones C3-1 and C3 develop at the elevations of 750–700 m. Fault F17, along the NE direction and with a high deep angle and a width of 1.2–3.0 m, obliquely cuts the dam foundation at an elevation of 680 m. The intraformational faulted zones with columnar jointing (i.e., LS3319, LS3320 and LS3320-1) play a significant role in these regions. Figure 1a shows a sketch of the main geological structures at the left bank slope.

2.2 Excavation Procedure and Observed Problems at the Left Bank Slope

The blasting excavation at the rock slope started on September 22, 2013, with the excavation elevation of 628 m on December 26, 2014. The foundation base of the dam located between the elevations of 834 and 660 m was completed, and the regions between the elevations of 660 and 650 m were the excavation experiment zones composed of basalt with columnar jointing and a 2-m-thick reserved protective layer. The reserved protective layer was 5 m deep between the elevations of 650 and 628 m. Figure 1a shows the excavation schedule of the rock slope.

Some sprayed concrete spalling, occurring at the peripheries of the entrances to the drainage tunnel PSL2 and the curtain grouting tunnel WML2 at an elevation of 654 m, was first discovered on December 13, 2014, as illustrated in Fig. 1a. A mortar strip was applied to the cracks on December 18, 2014; however, new ruptures and malpositions occurred at the mortar strips on December 23, 2014. In addition, cracking occurred at the side slope of the downstream spandrel groove along fault F17 on December 25, 2014, with an approximately 1-cm expansion on the top and 0.3-cm expansion at the toe of the slope, 1 m away from the dam foundation surface, as shown in Fig. 1a. Some explanations can be provided based on the geological data: the failure phenomena are mainly attributed to the combined actions of the shear deformation of LS3319 and the expansion deformation of fault F17. The block composed of these two faults could become loose if the deformation continued to develop, which would be detrimental to the anti-sliding stability of the dam abutment. Thus, the excavation activity of the dam foundation slope was suspended on December 29, 2014. The support measures were requested to be completed before February, 2015.

3 Characteristics of Microseismicity Measurement installed in the Left Bank Slope

3.1 MS Monitoring System

The MS monitoring system had been successfully implemented at the rock slope since November 10, 2014. A total of 18 uniaxial accelerometers with a natural frequency of 10 kHz deployed in boreholes drilled from the sidewalls of different tunnels (i.e., drainage tunnels and grouting tunnels) were installed. Figure 1b shows the spatial distribution of the sensor array. The fundamental principle and technical parameters of the MS monitoring technique are detailed in related studies (Trifu and Shumila 2010; Xu et al. 2012).

3.2 Spatiotemporal Distribution of Microseismicity at the Left Bank Slope

After filtering out the noisy events, 833 MS events were recorded within a given volume of interest during the selected period from November 10, 2014, to March 20, 2015. A plot of the cumulative number of MS events recorded during the selected period shows one period of increased MS activity, namely December 5, 2014, to January 10, 2015, as illustrated in stage “a” of Fig. 2. During stage “a”, there were approximately 13 MS events per day. This graph can be compared to the time history of excavated rock mass at the left bank slope (Fig. 1a). The graph shows that the curve of cumulative MS events in Fig. 2 exhibits almost the same tendency as the scheme of the excavated volume of rock mass (volume blasted) in Fig. 1a. According to on-site observations, the dam foundation slope, the drainage tunnel PSL4 and the curtain grouting tunnel WML4 at an elevation of 750 m were being excavated during this period. These excavation activities strongly contributed to the clustering of MS events in the time series. This is a good correlation and illustrates the strong consistency between the volume of rock mass being excavated and the total number of MS events. Therefore, excavation activities play a significant role in the levels of extension fracturing within a rock slope—the deeper the slope is, the more stressed it is and thus the more it fractures after being unloaded due to excavation (Xu et al. 2012). Another interesting phenomenon is that although excavation activities of the dam foundation slope were suspended on December 29, 2014, a number of MS events continued to occur in the rock slope between January 23 and March 20, 2015, as shown in stage “b” of Fig. 2. The following spatial distribution of MS events can be used to interpret the phenomenon.

Figure 3 shows the spatial distribution of MS events recorded during the selected period between November 10, 2014, and January 23, 2015. During this period, the rock

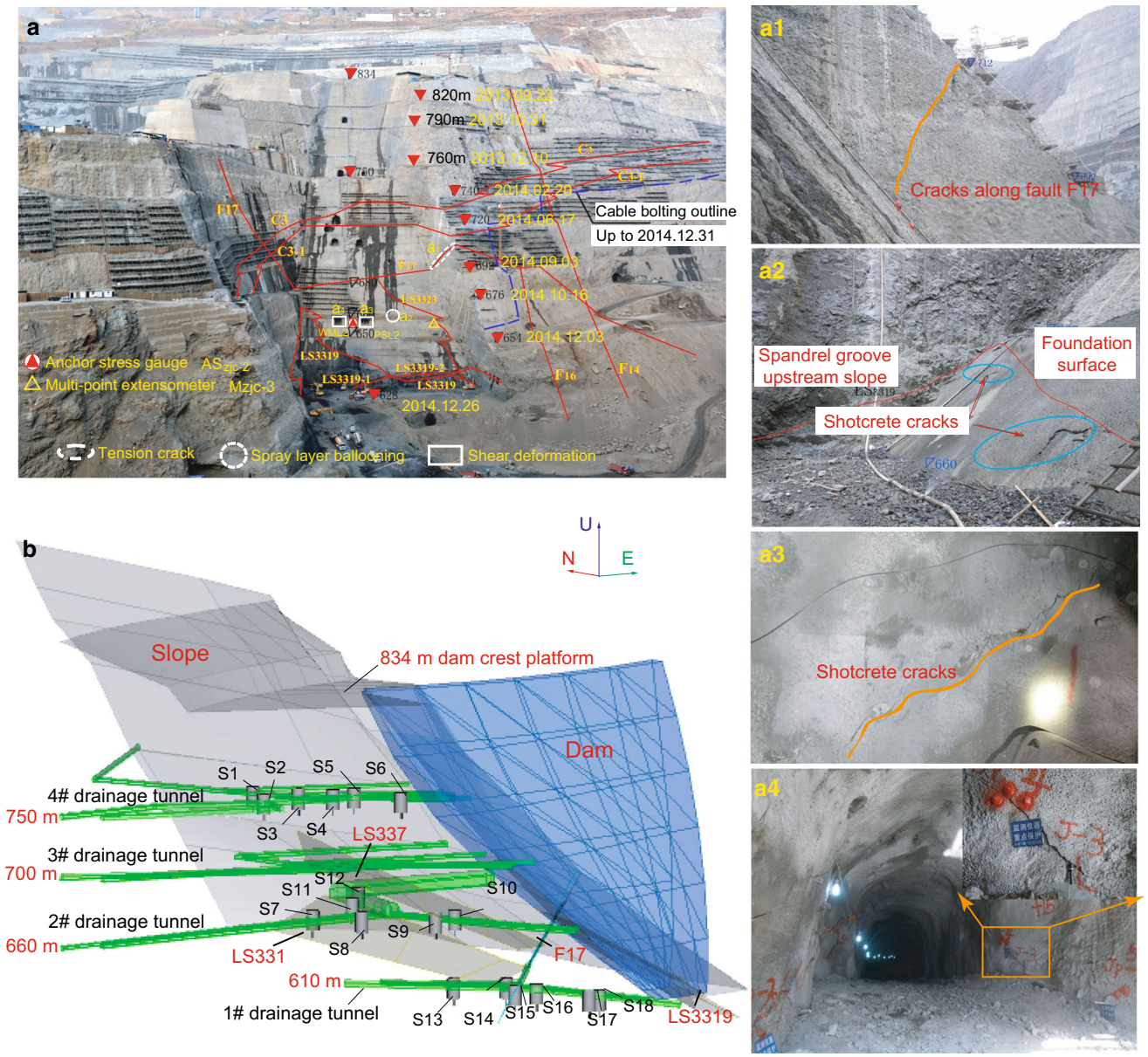

Fig. 1 **a** Sketch of geological structures at the left bank slope and **b** spatial arrangement of the sensor array (the columns represent different tunnels such as transportation tunnels, drainage tunnels and grouting tunnels). Herein, *a1–a4* are the different failure phenomena occurred at the rock slope. (*a1*) Cracks occurring along fault F17 at the downstream slope of the spandrel groove, (*a2*) sprayed concrete cracks at the upstream dam foundation, (*a3*) sprayed concrete cracks occurring at the sidewall of drainage tunnel PSL2 and (*a4*) sprayed concrete spalling occurring at the peripheries of the entrances to the curtain grouting tunnel WML2

slope was continuously excavated from elevations of 665 m to 628 m (until December 29, 2014), and the drainage tunnel PSL4 and curtain grouting tunnel WML4 at an elevation of 750 m were also excavated (through the end of January, 2015). The MS events show that these hypocenters were concentrated in the excavation zones (i.e., the slope of the dam spandrel groove, as shown in Fig. 3b) due to the excavation configuration. As illustrated in Fig. 3a, most of the MS events occurred at the bottom of the left bank slope, specially focusing on LS331 and LS337, as well as the hanging wall of fault F17, with elevations ranging from 610 to 700 m. The aerial view in Fig. 3b shows that MS events were being recorded at significant depths into the slope. However, a small number of MS events occurred at the top of the rock slope. This may be partly attributed to residual movements in the rock slope at high elevations and/or the excavation of shear-resistance tunnels. On the other hand, it may also be partly due to stress concentrations resulting from slope geometry. In addition, to highlight the relationship between the spatial distribution of MS events and the geological structure elements, Fig. 3c shows the released energy density

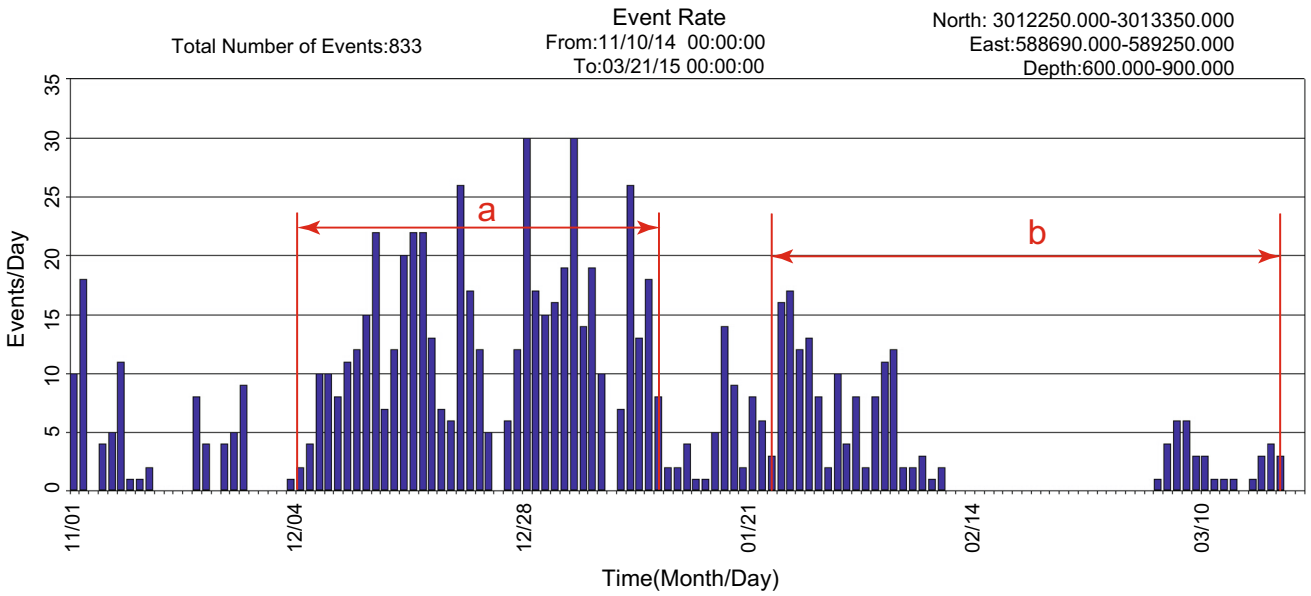

Fig. 2 Temporal distribution of MS events during the selected period between November 10, 2014, and March 20, 2015

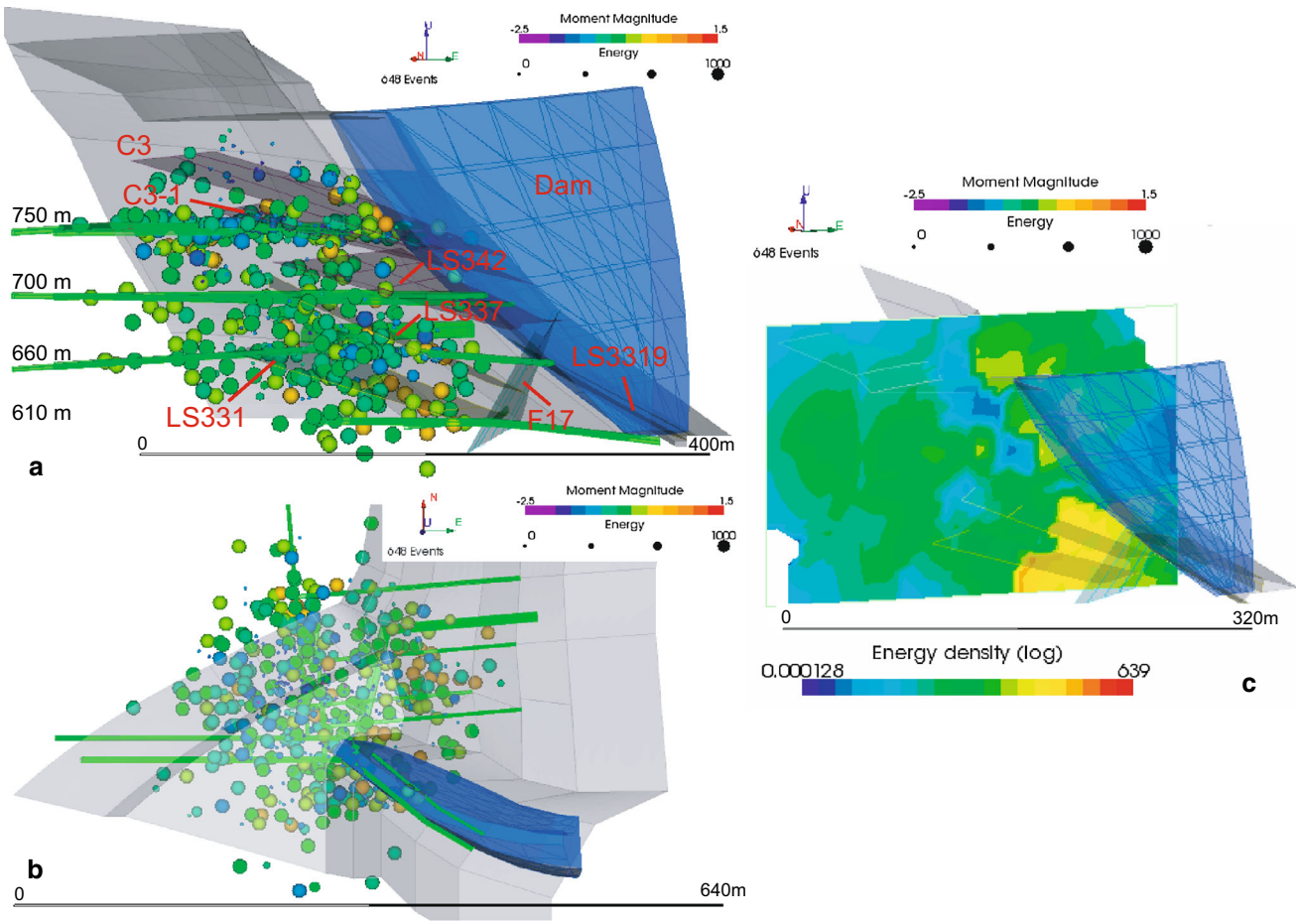

Fig. 3 Spatial distribution of MS events during the selected period between November 10, 2014, and January 23, 2015. **a** Front view, **b** aerial view and **c** energy density contour of MS events. The *colors of the spheres* in the figures indicate different moment magnitudes, and the *sphere size* is proportional to the energy scale (colour figure online)

contours of seismic source locations. MS events show a strong correlation with structural elements on-site, particularly with LS331, LS337 and fault F17. Thus, the potential risky regions in the left bank slope, where microseismicity is active or inactive, can be identified.

Further, Fig. 4 shows the spatial distribution of MS events that occurred in the rock slope during the selected period between January 24 and March 20, 2015. A number of MS events remained concentrated along LS331 and LS337 even though the excavation activity of the dam foundation slope was suspended on December 29, 2014. Similarly, Fig. 4c shows the seismic deformation contours of MS events, therein highlighting the correlation between microseismicity and structure elements (i.e., LS331 and F17). According to construction activities and field observations, this clustering was mainly caused by the combined actions of the shear deformation of the intraformational faulted zones (i.e., LS331 and LS337) and the expansion deformation of fault F17 after the latter was exposed at the toe of the dam foundation slope. The evolutionary characteristic of MS events in the rock slope is acted on by both external and internal sources. The former is the excavation-induced unloading effect, and the latter consists of preexisting weak structural planes.

3.3 Correlation Among MS Activity, Conventional Testing and Field Observation

To analyze the correlation between conventional measurement and MS monitoring methods, some typical monitoring data such as anchor stress gauges and multi-point extensometers at a typical elevation of the rock slope were selected to compare with the microseismicity. The arrangement of conventional measuring apparatuses (i.e., anchor stress gauge and multi-point extensometer) is shown in Fig. 1a. Figure 5a shows the absolute displacement process graph of the Mzjc-3 multi-point extensometer at the dam foundation at an elevation of 654.53 m. The increase in the displacement during the second half of December 2014 is a result of production blasts during rock slope excavation. By comparing Fig. 5a with Fig. 2, a similar growth trend is obtained during the second half of

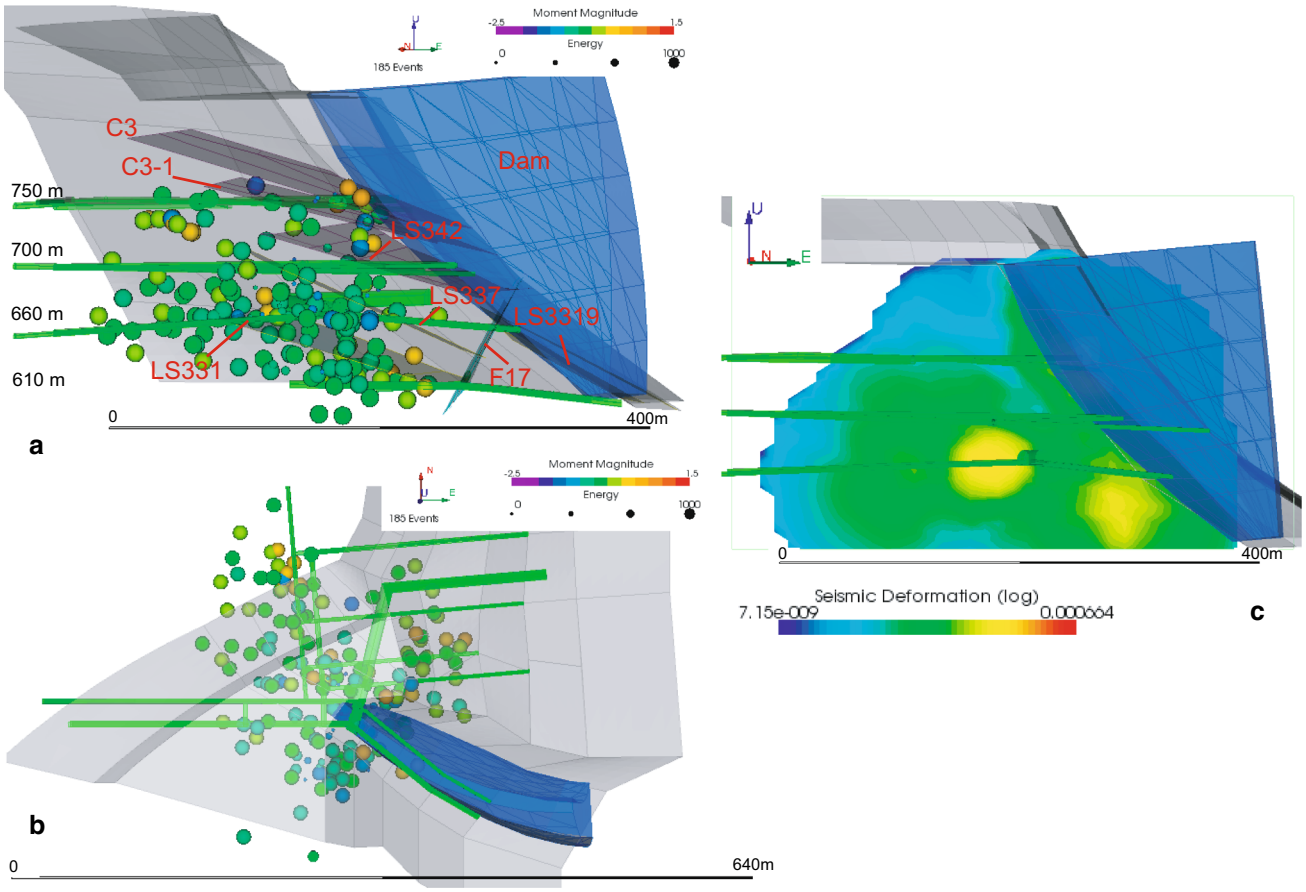

Fig. 4 Spatial distribution of MS events during the selected period between January 24 and March 20, 2015. **a** Cross-section looking along the east–north projection, **b** top view and **c** seismic deformation contour of MS events from south–north vertical cross-section looking east

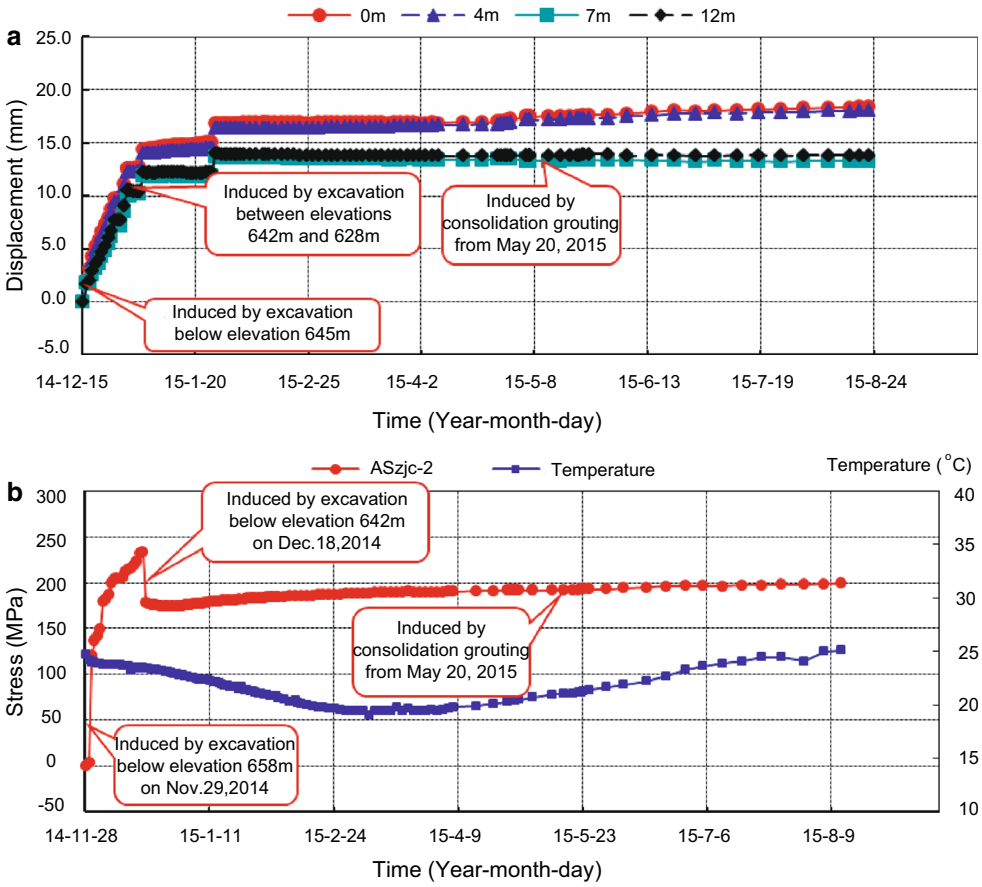

Fig. 5 **a** Absolute displacement process graph of the Mzjc-3 multi-point extensometer in the experimental zone of the columnar jointing at the dam foundation at an elevation of 654.53 m and **b** stress process graph of the ASzjc-2 anchor stress gauge in the experimental zone of the columnar jointing at the dam foundation at an elevation of 658.55 m

December 2014, in particular at the end of the month. The same change is attributed to production blasts during excavation of the dam foundation slope according to field observations and construction notes. However, it is worth noting that only a relative displacement of 5 mm occurred somewhere between depths of 4 and 7 m from the slope surface. This is mainly attributed to the length (only 12 m) of the multi-point extensometer installed in the zone. The deformation of the deep rock mass of the left bank dam foundation slope thus cannot be obtained. In addition, to study the stress redistribution induced by excavation of the dam foundation slope, a stress process graph of the ASzjc-2 anchor stress gauge (see Fig. 1a) at an elevation of 658.55 m is shown in Fig. 5b. The graph partly reflects the stress variation in anchor bolts in the deep rock mass of the spandrel groove slope. In contrast, unlike the results shown in Fig. 5a, the data obtained by the ASzjc-2 anchor stress gauge decreased on December 18, 2014. This can be used to accurately interpret the stress release mechanism induced by energy loss from MS events concentrated in the rock slope. Thus, MS activity can be regarded as the precursor to the surface deformation and even instability failure of the rock slope. The evolution of stress variation in processes leading to potential slope instability is consistent with the tempo-spatial distribution of MS events (Xu et al. 2012).

Moreover, to investigate the correlation between the MS activity and rock mass damage of the rock slope, field observations were frequently conducted. Some cracks were discovered in the past few months during continuous excavation of the rock slope, as shown in Fig. 1a. Figure 6 shows the comparison between the clustering of MS events and surface cracks in the rock slope. These cracks are mainly distributed around the spandrel groove slope of the arch dam, exactly above the excavation regions of the rock slope (Fig. 6d). With respect to the depths of MS events (Figs. 3, 4), the MS monitoring study conducted at the rock slope demonstrates that most of the MS events may be attributed to shear fractures between the different staggered zones (i.e., LS331, LS337 and C3-1) and tension cracking of faults (i.e., F17) induced by excavation unloading at the bottom of the dam foundation slope. Note that, right before the apparent field observation of surface cracks (see Sect. 2.2), the MS events had already accumulated significantly at different staggered zones (Figs. 3, 4); the occurring time of these surface cracks usually lags behind that of clustering MS events.

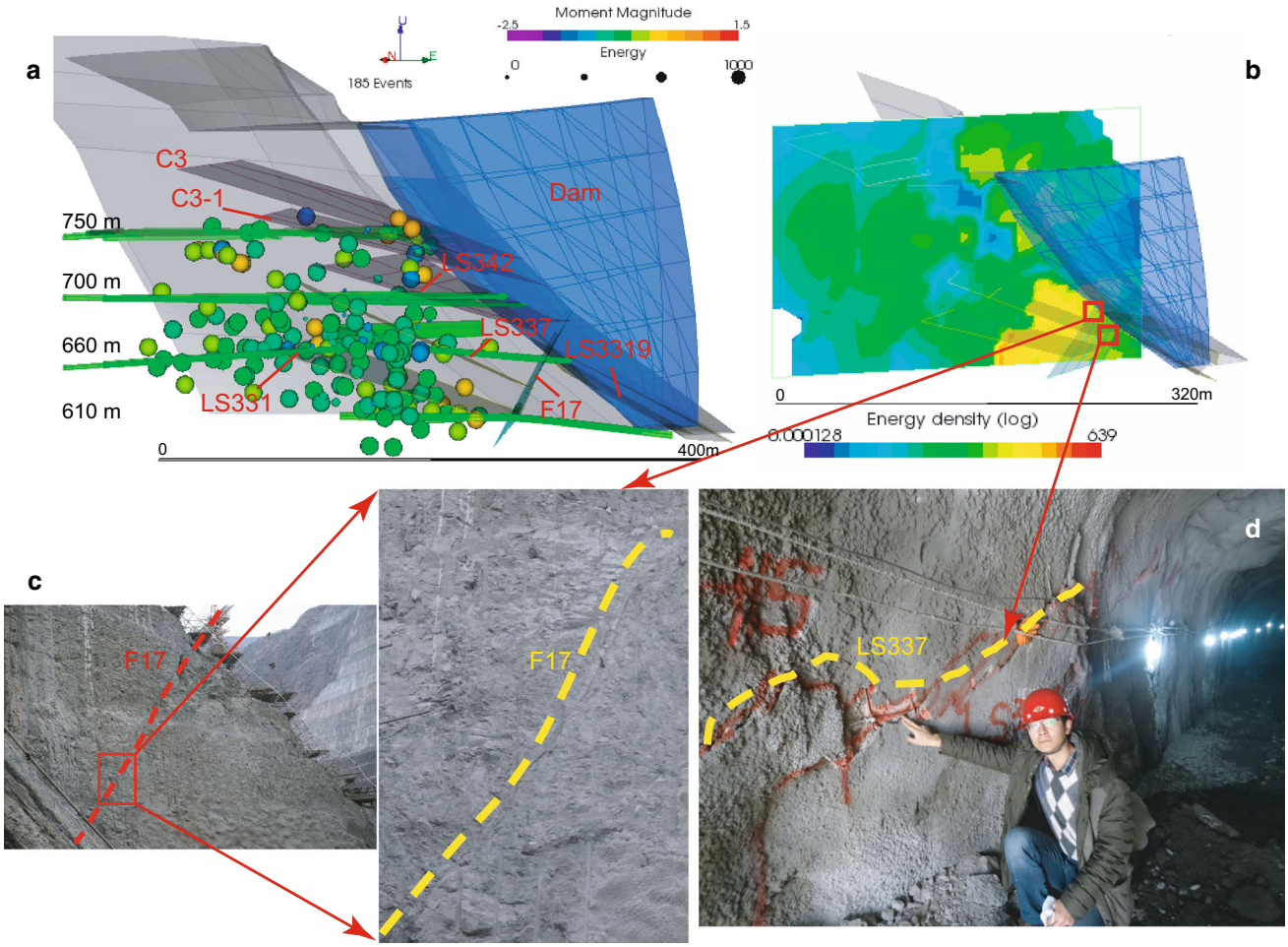

Fig. 6 Comparison between the clustering of MS events and surface cracks in the rock slope. **a** Spatial distribution of MS events, **b** energy density contour of MS events, **c** cracking occurring along fault F17 and **d** sprayed concrete spalling occurred along LS337 in the curtain grouting tunnel WML2

4 Concluding Remarks

In this study, a MS monitoring system was successfully implemented at the left bank slope at the Baihetan hydropower station. Real-time monitoring and analyses of rock mass damage subject to excavation in the rock slope were realized. The tempo-spatial evolution characteristics of microseismicity are observed closely related to the excavation dynamics of the rock slope. MS monitoring results can thus be used to delineate the micro-fracture clustered regions and potential sliding surfaces in the rock slope, as well as clearly illustrate the simultaneous activity characteristics of the preexisting weak geological structures. The integrated approach combining MS monitoring, traditional surveying and field observations leads to a better understanding of the excavation behavior of rock slopes and more effective references for construction schemes and supporting measures under complex geological and excavation conditions.

Acknowledgments The authors are grateful for the financial support from the National Program on Key basic Research Project (No. 2015CB057903), National Natural Science Foundation of China (51374149) and the Youth Science and Technology Fund of Sichuan Province (2014JQ0004). The authors would like to thank two anonymous reviewers for their valuable comments to improve this manuscript.

References

Cai M, Kaiser PK, Martin CD (2001) Quantification of rock mass damage in underground excavations from microseismic event monitoring. Int J Rock Mech Min Sci 38:1135–1145. doi:10.1016/S1365-1609(01)00068-5

Hirata A, Kameoka Y, Hirano T (2007) Safety management based on detection of possible rock bursts by AE monitoring during tunnel excavation. Rock Mech Rock Eng 40(6):563–576. doi:10.1007/s00603-006-0122-7

Hudyma M, Potvin YH (2010) An engineering approach to seismic risk management in hardrock mines. Rock Mech Rock Eng 43:891–906. doi:10.1007/s00603-009-0070-0

Kaiser PK (2009) Seismic hazard evaluation in underground construction. In: Tang CA (ed) Proceedings of the 7th international symposium on rockburst and seismicity in mines (RaSiM7), Dalian, China, 20–23 August 2009. Rinton Press, New York, pp 1–26

Liu YQ, Li HB, Zhao J, Li JR, Zhou QC (2004) UDEC simulation for dynamic response of a rock slope subject to explosions. Int J Rock Mech Min Sci 41(suppl 1):599–604. doi:10.1016/j.ijrmms.2004.03.106

Liu YQ, Li HB, Xiao KQ, Li JC, Xia X, Liu B (2014) Seismic stability analysis of a layered rock slope. Comput Geotech 55:474–481. doi:10.1016/j.compgeo.2013.10.002

Stacey TR, Wesseloo J, Lynch R (2004) "Extension" and seismicity in a hard rock open pit mine. In: Proceedings 2nd international seminar on deep and high stress mining, South Africa, South African Institute of Mining and Metallurgy, pp 41–53

Stead D, Wolter A (2015) A critical review of rock slope failure mechanisms: the importance of structural geology. J Struct Geol 74:1–23. doi:10.1016/j.jsg.2015.02.002

Stead D, Eberhardt E, Coggan JS (2006) Developments in the characterization of complex rock slope deformation and failure using numerical modelling techniques. Eng Geol 83:217–235. doi:10.1016/j.enggeo.2005.06.033

Tang CA, Wang JM, Zhang JJ (2011) Preliminary engineering appliction of microseismic monitoring technique to rockburst prediction in tunneling of Jinping II project. J Rock Mech Geotech Eng 2(3):193–208

Trifu CI, Shumila V (2010) Microseismic monitoring of a controlled collapse in field II at Ocnele Mari, Romania. Pure appl Geophys 167:27–42. doi:10.1007/s00024-009-0013-4

Wang XB, Jin K, Yao W, Zhao FT, Tian XX, Fan XW, Du JL, Zhao ZY (2015) Report on engineering geology of deformation treatment of the left bank dam foundation and dam abutment slope at the elevation of 720 ~ 628 m of the Baihetan hydropower station along Jinshajiang River. Hangzhou: PowerChina Huadong Engineering Corporation Limited, Hangzhou, China, pp 147 (in Chinese)

Xu NW, Tang CA, Li H, Dai F, Ma K, Shao JD, Wu JC (2012) Excavation-induced microseismicity: microseismic monitoring and numerical simulation. J Zhejiang Univ Sci A (Appl Phys Eng) 13(6):445–460

Xu NW, Dai F, Liang ZZ, Zhou Z, Sha C, Tang CA (2014) The dynamic evaluation of rock slope stability considering the effects of microseismic damage. Rock Mech Rock Eng 47:621–642. doi:10.1007/s00603-013-0432-5

Xu NW, Li TB, Dai F, Zhang R, Tang CA, Tang LX (2016) Microseismic monitoring of strainburst activities in deep tunnels at the Jinping II hydropower station, China. Rock Mech Rock Eng 49:981–1000. doi:10.1007/s00603-015-0784-0

Young RP, Collins DS, Reyes-Montes JM, Baker C (2004) Quantification and interpretation of seismicity. Int J Rock Mech Min Sci 41:1317–1327. doi:10.1016/j.ijrmms.2004.09.004